JOURNAL OF MATERIALS SCIENCE **34** (1999) 379–384

Change of mechanical properties of rigid poly(vinylchloride) during photochemical ageing

C. ANTON-PRINET, G. MUR
RHÔNE-POULENC, 52, rue de la Haie Coq, 93308 Aubervilliers Cédex

M. GAY
RHÔNE-POULENC, 85 avenue des frères Peret, 69192 Saint-Fons Cédex

L. AUDOUIN*, J. VERDU
ENSAM, 151 boulevard de l'hôpital, 75013 Paris

Thermally stabilised, unpigmented, rigid PVC samples, were exposed to accelerated photoageing at 40 °C, 55 °C and 70 °C. The concentration profiles of photoproducts were determined on microtome slices ($\sim 20\,\mu$m) parallel to the irradiated surface using IR (carbonyls) and UV (polyenic double bonds) spectrophotometry and by steric exclusion chromatography (M_n and M_w). They indicate that carbonyls and chain scissions predominate only in a thin superficial layer whereas polyconjugated double bonds and crosslinks predominate in a subcutaneous layer (~ 300–$400\,\mu$m). Tensile measurements show that the ultimate elongation decreases after an induction period whose duration is a decreasing function of temperature. The change of mechanical behaviour can be described in terms of a ductile-brittle transition shift mechanism in which crosslinking plays an important role. A tentative explanation of a such crosslinking induced transition is proposed in the discussion.

1. Introduction

There is a great technical and economical interest for building applications (for instance windows) of rigid PVC since about 30 years. It is well known that PVC is intrinsically sensitive to photochemical ageing, which leads to its discoloration and embrittlement, both phenomena being not necessarily interrelated. There is no consensus on degradation mechanisms despite the impressive amount of published data [1–3]. However, the problem of weatherability has been more or less empirically solved, using "try and error" procedures, by progressive modifications of the formulation in which the thermal stabilisation system and the pigment nature (essentially surface treated TiO_2) dispersion and concentration play a role. These choices are, however, periodically questioned for economical or environmental reasons, for instance the Lead being replaced by non toxic systems such as Calcium-Zinc ones. The long term stability of the new systems is indeed to be experimentally proved which revives the interest on the degradation mechanism.

The present article deals with the embrittlement mechanism induced by photoageing in PVC. Despite the relatively abundant literature published on this topic in the past decades [4–10], it seemed interesting to us to reconsider the problem on the basis of new concepts appeared in the eighties [11–13], using the recent advances in the field of polymer physics and fracture mechanics. The new vision of the problem attaches for instance a peculiar importance to the thickness profile of the degradation products, but efficient experimental methods to determine this latter have been essentially developed in the last decade [14]. As it has been shown recently [15, 16], the case of PVC is especially complicated because the degraded zone is composed of two layers of very distinct characteristics: the superficial layer, in which oxidation products and chain scission predominate, and the subcutaneous layer in which HCl elimination products (conjugated polyenes) and crosslinking predominate. This "macrostructure" is practically independent of exposure conditions [17]. It has been explained by the fact that polyenes and alkyl radicals (responsible for crosslinking) can survive only in conditions of kinetic control by oxygen diffusion, i.e. at a certain distance of the exposed surface [16].

The aim of this article is to try to determine the eventual influence of this peculiar structure on the embrittlement process.

2. Experimental

2.1. Material

An industrial PVC sample ($M_n = 90\,\text{kg mol}^{-1}$, $M_w = 200\,\text{kg mol}^{-1}$) thermally stabilised by a Calcium-Zinc-β-dicetone ternary mixture, free of pigments and light stabilisers, was used in this study. The polymer

* Author to whom all correspondence should be addressed.

powder was premixed with additives at 1800 rotations per minute at 100 °C during 15 min. Ribbons of 1 mm thickness were made from this mixture by extrusion using a monoscrew extruder working in 170–200 °C temperature range.

Tensile samples (according to the French Standard NFT 51034) were cut in the longitudinal direction of the ribbons.

2.2. Exposure

The samples were exposed in photochemical reactors equipped with fluorescent lamps Philips TKL 5, 40 W ($300\,\text{nm} < \lambda < 450\,\text{nm}$, $\lambda_{max} = 365\,\text{nm}$) with an intensity of $7 \cdot 10^{18}$ photons $\text{cm}^{-2}\ \text{h}^{-1}$ at the sample surface. These experiments were made at respectively 40 °C, 55 °C and 70 °C.

2.3. Sample testing

Periodically, five samples were taken for physicochemical and tensile measurements. The depth distribution of photoproducts was established from IR, UV and GPC measurements on microtome slices ($\sim 20\,\mu$m thickness) parallel to the irradiated surface.

Infrared measurements were made using a Bruker IFS 28 spectrophotometer. The absorbance A_{CO} was determined at the maximum of the carbonyl band ($\sim$1720 cm^{-1}). The results were expressed in terms of carbonyl concentration $[CO] = A_{CO}/\varepsilon_{CO}\ L$ (mol l^{-1}), L being the film thickness and ε_{CO} the molar absorptivity of carbonyl groups. This latter can vary between about 190 and 500 1 $\text{mol}^{-1}\ \text{cm}^{-1}$ depending on the carbonyl structure. A value of 300 1 $\text{mol}^{-1}\ \text{cm}^{-1}$ has been arbitrarily taken in order to obtain the order of magnitude of the carbonyl concentration.

UV measurements were made using a Perkin Elmer Lambda 5 apparatus. The absorbance A_u was determined at the maximum of the large band ($\lambda_{max} \sim$ 500 nm) corresponding to the carotenoïd polyenes (P_n) (10–12 conjugated double bonds). Their concentration (in mol l^{-1}) was estimated using:

$$[P_n] = A_u/\varepsilon_u L$$

ε_u being the molar absorptivity of the polyenes. This method can give only the order of magnitude of the concentration, owing to the overlapping of the spectra of polyenes. The chosen value of ε_u was $3.2 \cdot 10^5$ l mol^{-1} cm^{-1} according to literature on model compounds [18].

Average molar masses M_n and M_w were determined from steric exclusion chromatographic measurements using tetrahydrofurane as solvent. Details on the measurement method will be published elsewhere [16]. It will be only recalled here that M_n values are relatively accurate, whereas M_w values are only valid to indicate a trend because of the possible presence of an insoluble fraction in the subcutaneous layer.

Mechanical measurements were made only on bulk samples. DMTA measurements were made in the flexural configuration using a Polymer Laboratories apparatus at 1 Hz frequency between 50 °C and 140 °C. Tensile measurements were made at ambient temperature, at 15 mm min^{-1} deformation rate using an INSTRON 4301 dynamometer and the ultimate coordinates σ_R (stress) and ε_R (elongation) were recorded.

3. Results

The depth profiles of carbonyl concentration, polyene concentration and average molar weight are shown respectively in Figs 1–3 in the case of a sample irradiated

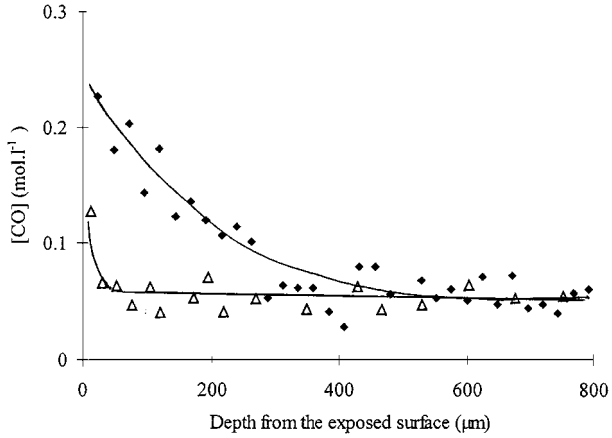

Figure 1 Carbonyl concentration profile for a bulk rigid PVC sample △ unexposed and ♦ irradiated for 450 h at 70 °C.

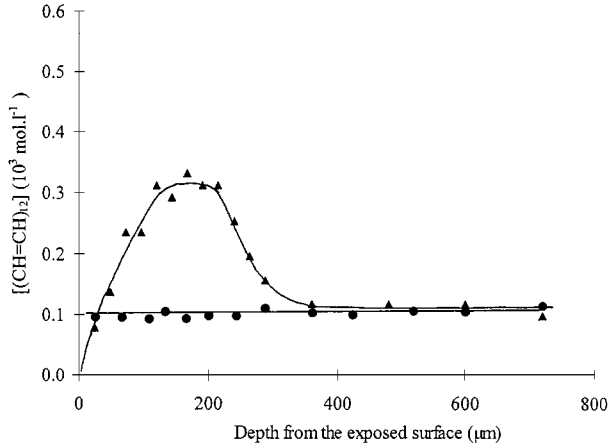

Figure 2 Polyene concentration profile for a bulk rigid PVC sample ● unexposed and ▲ irradiated for 450 h at 70 °C.

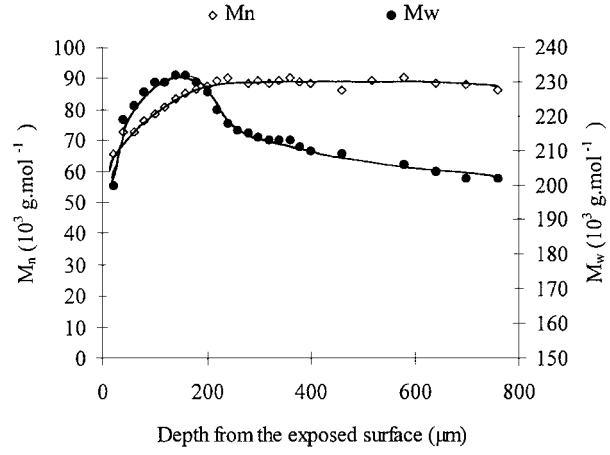

Figure 3 Molecular weight profile for a bulk rigid PVC sample irradiated for 450 h at 70 °C.

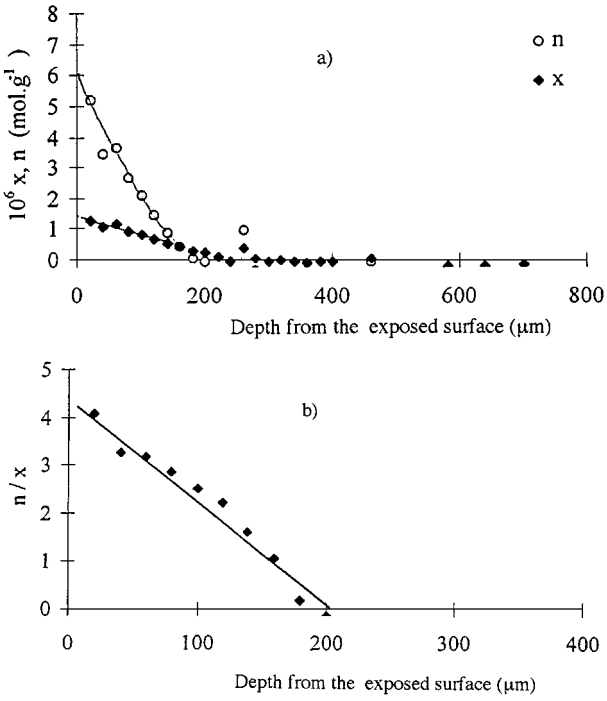

Figure 4 Depth profiles of (a) chain scission n and crosslinks x and (b) n/x in the PVC bulk sample irradiated for 450 h at 70 °C.

450 h at 70 °C. The same shape of photoproducts depth distribution has been observed in all the other experimental conditions under study, with only small qualitative variations [17]. The relatively low influence of exposure conditions on degradation profiles has been explained elsewhere from kinetic considerations [19]. It appears that oxidation products are concentrated in a relatively sharp skin layer ($x < 100\ \mu$m). Numbers of moles of chain scissions n and crosslinks x per mass unit (calculated using Saïto equations [20]) were plotted against sample depth as well as the ratio n/x (Fig. 4a and b). The ration n/x decreases almost linearly with depth, showing that crosslinking predominates in most of thickness of degraded layer. It is higher than 4 (chain scissions predominate to crosslinking) only in a thin superficial layer which agrees with recently published results obtained on thin films [21]. Beyond a depth of about 50 μm, conjugated polyenes accumulate with a maximum concentration near to 200 μm. Their concentration decreases from this maximum to about 400 μm which corresponds to the limit of the photodegraded zone and beyond which the polymer keeps its initial characteristics. The layer in which M_w is higher than its initial value, i.e. in which crosslinking predominates over chain scission corresponds more or less to the layer where polyenes are present.

Mechanical testing leads to observations previously made by various research groups [4–10]:

- There is practically no change of the mechanical behaviour at small deformations. Modulus changes are insignificant over the whole exposure time whatever the temperature.
- In contrast, the ultimate properties undergo strong variations.
- Ageing affects essentially the elongation at break ε_R. The variation of the stress at break σ_R is determined by the behaviour law $\sigma = f(\varepsilon)$ of the polymer (ε and σ being respectively elongation and stress) and this latter remains unchanged by ageing. In other words, the rupture envelope $\sigma_R = f(\varepsilon_R)$ corresponds to the initial tensile curve $\sigma = f(\varepsilon)$ (Fig. 5), which seems to be a very general rule in polymer ageing [8–13]. This means that globally, the material undergoes only few modifications but defects accumulate, so that the elongation at break decreases.

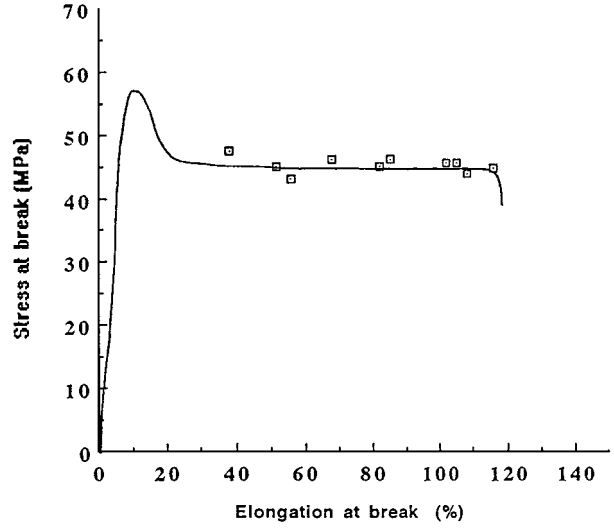

Figure 5 Rupture envelope for a rigid PVC photoageing at 70 °C.

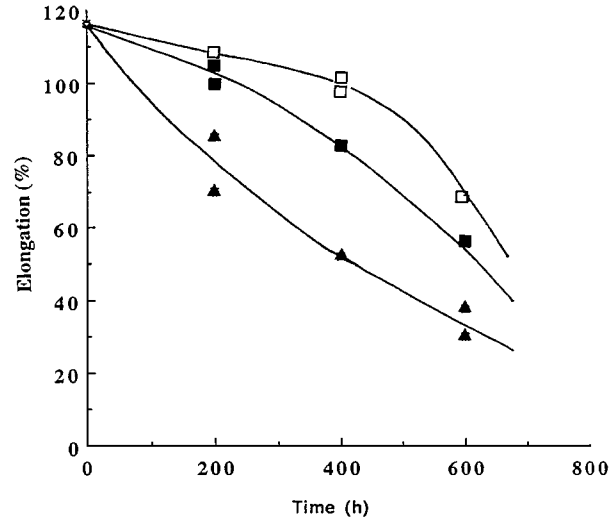

Figure 6 Kinetic curves of ultimate elongation changes during photochemical ageing at different temperatures: ▲ 70 °C, ■ 55 °C, □ 40 °C.

The kinetic curves of ultimate elongation changes are presented in Fig. 6. At low exposure temperate, they display an initial plateau, followed by a more or less sharp decrease, and then a final plateau where the ultimate elongation is close to the initial elongation at yield ε_{y_0}. This behaviour can be assimilated to a ductile-brittle transition spread over time. The initial plateau is due to the fact that ageing kinetics display an induction period linked to the stabiliser consumption. Unstabilised samples are, however, expected to display also an initial plateau corresponding to the time needed to reach the initial structural state at which ductile-brittle transition occurs. Ultimate elongation tends to a final

plateau is due to the fact that in brittle regime, when plastic deformation becomes negligible, the ultimate stress becomes practically independent of the macromolecular scale structure (chain length, crosslinking density) but depends essentially of the cohesion and defect geometry, both properties being modified only very slowly by ageing. Taking an arbitrary endlife criterion $\varepsilon_R = 2/3\varepsilon_{R_0} = 80\%$, one obtains the following values for the lifetime t_F, $t_F = 150$ h at 70 °C, 350 h at 55 °C and 500 h at 40 °C. It appears thus that temperature is a key factor in accelerated PVC photochemical ageing. At 70 °C, the induction period is practically reduced to zero so that the shape of ageing curve is not the same as at 55 and 40 °C. The lifetime t_F seems to obey the Arrhenius equation $\ln t_i = -7.305 + 4257\ T^{-1}$ with $R = 0.966$, the apparent activation energy being about 35 kJ mol^{-1}.

4. Discussion

Embrittlement during polymer ageing is usually attributed to chain scission. When the molecular weight becomes lower than a critical value M_c, which is of the order of 10 kg mol^{-1}, the entanglement network is destroyed, plastic deformation cannot occur and the toughness decreases sharply of two or three orders of magnitude [22]. Cracks propagate rapidly in the oxidized layer. This latter can be considered more or less as a defect able (beyond a critical size) to initiate the sample fracture. This behaviour can be predicted from fracture mechanics considerations [23]. In the case under study, however, the minimum value of molar mass M_{ns} (in the superficial layer), remains noticeably higher than $M_c : M_{ns} > 50$ kg mol^{-1} against $M_c < 10$ kg mol^{-1}. Furthermore, the oxidized layer in which there is a molar mass decrease is very thin, typically less than 50 μm, so that its "sensitizing effect" on fracture must be limited. We have thus to try to imagine another embrittlement mechanism than chain scission and this leads in our case to consider the role of crosslinking.

The thickness of the crosslinked zone is about 400 μm, which constitutes a defect size in principle sufficient to initiate the sample fracture, but does crosslinking lead to embrittlement? It is generally positively answered to this question on the basis of rubber elasticity considerations. Now it is well recognised that the rubber elasticity theory can be used to model the plastic deformation of thermoplastics [24]. In the frame of this theory, the ultimate elongation ε_R, or better the ultimate draw ratio $\Lambda_R = 1 + \varepsilon_R$, is a decreasing function of the crosslink density. In an ideal case, we would have: $\Lambda_R = C M_E^{1/2}$, where C is a constant depending essentially on the chain characteristic ratio C_∞ [25] and M_E is the molar mass of elastically active chains. In this case, the decrease of Λ_R is expected to be progressive and accompanied by an increase of the ultimate stress, which is not observed in our case.

Another way of interpretation consists to consider the change of ultimate properties as a result of ductile-brittle transition. The corresponding transition temperature, initially lower than the ambient temperature, would increase progressively as a result of crosslinking. So that the initially ductile samples would progressively become brittle (Fig. 7). But how to explain the relationship between crosslinking and ductile-brittle transition? DMTA results (Fig. 8 and Table I) indicate that T_g increases, which constitutes a possible way of explanation. Flexural loading is especially sensitive to superficial changes of the stiffness. But, the transition temperature measured by this method is a complex function

TABLE I Solubility in THF and T_g (determined using DMTA) of rigid PVC samples during photoageing at different exposure times and temperatures

Samples	T_g (°C)	Solubility in THF
Virgin	89	Yes
600 h at 55 °C	89	Yes
600 h at 70 °C	95	No
1150 h at 70 °C	94	No

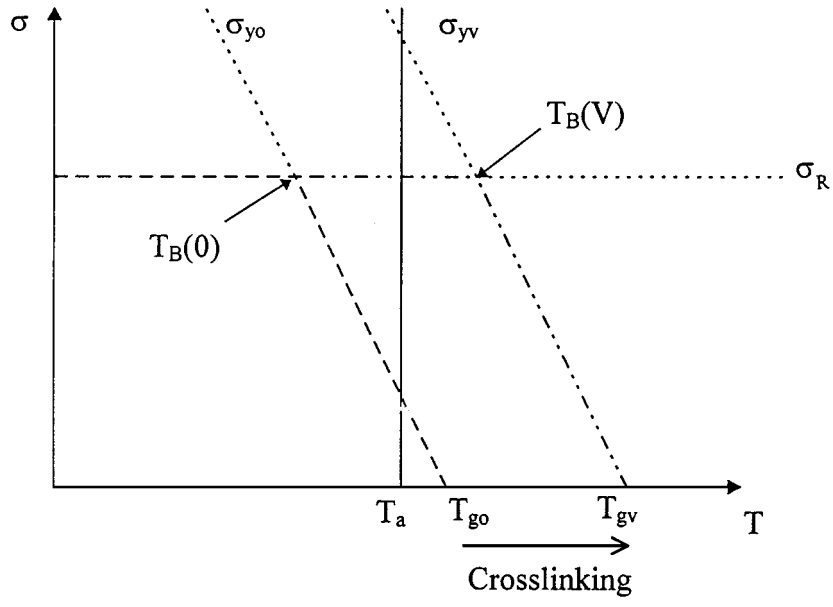

Figure 7 Schematisation of ductile-brittle transition shift owing to crosslinking, where T_B is a ductile-brittle transition temperature, T_g a glass transition temperature, T_a is an ambient temperature; signs (o) and (v) are relatives to unexposed and photodegraded samples respectively; σ_y and σ_R are yield stress and ultimate stress respectively.

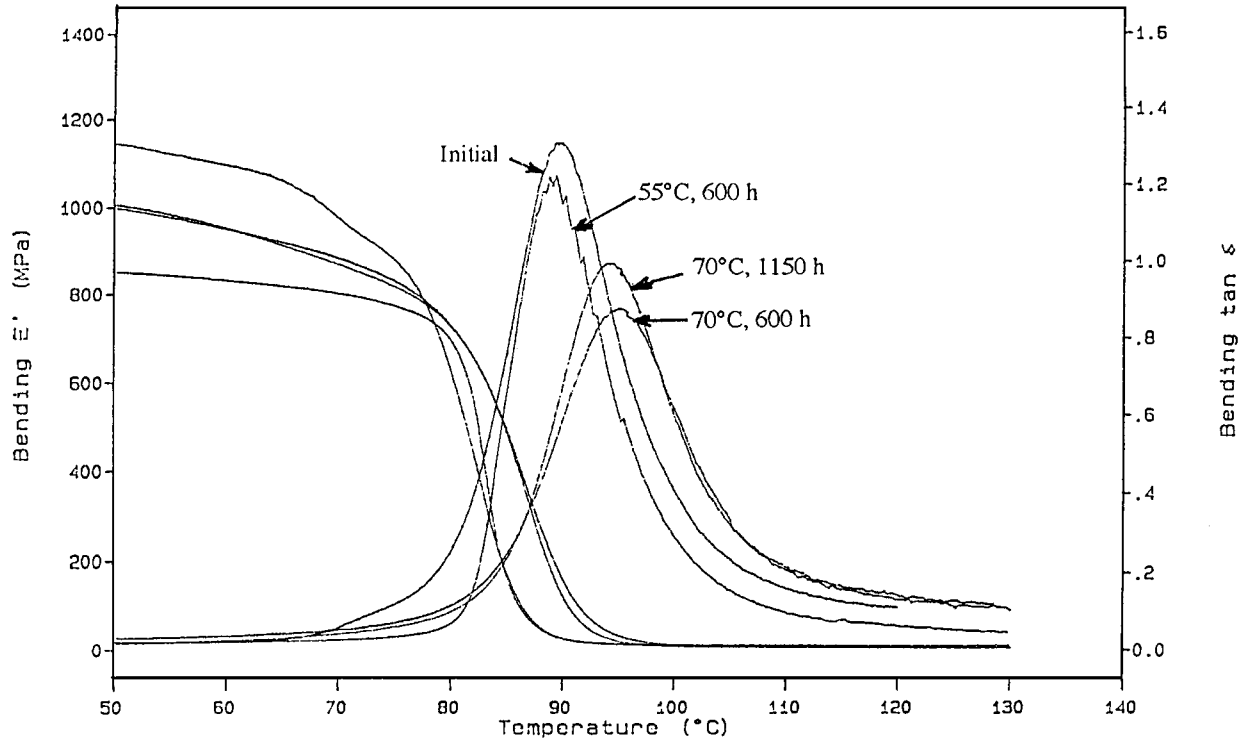

Figure 8 DMTA measurements in flexural configuration at 1 Hz frequency between 50 and 140 °C for the bulk rigid PVC samples after photoageing at different conditions.

of the spatial distribution of local T_g values in superficial layers and it is lower than the maximum T_g value corresponding presumably to the layer of maximum crosslink density near to 200 μm depth. The experimental value of T_g determined by DMTA can be thus associated to a mean value of the crosslink density of the whole sample which can be considered as an underestimate of the local maximum crosslink density.

The theoretical crosslink density n can be estimated from the Di Marzio's relationship [26]:

$$T_g = \frac{T_{gl}}{1 - KnF}$$

where T_{gl} is the T_g of the uncrosslinked PVC, K is a universal constant. $F = m/\gamma$, where $m = 62.5$ g mol^{-1} for PVC is the molar mass of the monomer unit, and γ (2 for PVC) is the number of rotatable bonds in the monomer unit. n is the crosslink density expressed for instance in terms of the network nodes concentration:

$$n = \frac{2}{fM_E}$$

where f is the node functionality ($f = 4$ in the case under study). Considering that $K/f \sim 1$ and N_E is the number of monomer units per network strand, Di Marzio's relationship can be thus written:

$$T_g = \frac{T_{gl}}{1 - [K \cdot (m/2) \cdot (2/fM_E)]} = \frac{T_{gl}}{1 - [(K/f) \cdot (1/N_E)]} \quad N_E = \frac{M_E}{m}$$

$$T_g = \frac{T_{gl}}{1 - (1/N_E)}$$

So that:

$$N_E = \frac{T_g}{T_g - T_{gl}}$$

Using $T_g = 95\,^\circ$C (Table I) we obtain $N_E \sim 60$ after 600 h at 70 °C, which would correspond to a crosslink density of the order of magnitude of the entanglement density. In fact, local crosslink densities can be higher than this value.

Let us now consider the ductile-brittle transition as the result of a competition between a brittle mechanism characterised by an ultimate stress σ_R almost independent of the temperature, and a ductile mechanism characterised by its yield stress σ_y (Fig. 8). For linear polymers, σ_y varies almost linearly with temperature [27].

$$\sigma_y = A(T_g - T) \quad \text{(where } A \text{ is constant)}$$

so that the ductile-brittle transition temperature T_B is given by:

$$\sigma_R = A(T_g - T_B)$$

and

$$T_B = T_g - \sigma_R/A$$

Progressive embrittlement results from an increase of T_B (which is initially lower than ambient temperature), which in turn can result:

1. From an increase of T_g, σ_R and A being constant as illustrated in Fig. 6.
2. From a decrease of σ_R, but this latter is expected to depend essentially on the cohesive energy density

which must vary significantly only at relatively high conversions.

3. From an increase of A which is also linked to the cohesive energy density [27] and to intramolecular energy barriers [28]. It is noteworthy that Kambour's law can be derived from the Eyring's equation:

$$\varepsilon_y = \varepsilon_0 \cdot \exp -\frac{(Q - V\sigma)}{RT} \quad (Q \text{ and } V \text{ are constants, for more details see [27]})$$

In this case, A could be:

$$A = \frac{R}{V} \ln \frac{\varepsilon_y}{\varepsilon_0}$$

Unfortunately, little is known on the effect of crosslinking on the Eyring's parameters, although data on epoxy networks seem to indicate that V is a decreasing function of the crosslink density, i.e., A is an increasing function of the crosslink density [29]. It seems thus reasonable to explain the embrittlement of PVC during its photochemical ageing by the occurrence of crosslinking in a subcutaneous layer. Crosslinking induces an increase of T_g and, presumably, an increase of the slope

$$A = \frac{d\sigma_y}{dt}.$$

Both phenomena contribute to increase the brittle transition temperature T_B. Embrittlement begins when this latter approaches the temperature at which mechanical properties are measured.

References

1. Review in W. H. STARNES, "Developpements in Polymer Degradradation," Vol. 3, edited by N. GRASSIE (Applied Science Publishers, London, 1981) pp. 135–173.
2. R. BACALOGLU and M. FISCH, *Polym. Deg. Stab.* **45** (1994) 301.
3. B. D. GUPTA and J. VERDU, *J. Polym. Eng.* **8** (1988) 73.
4. G. ROUX and P. EURIN, *J. Macromol. Sci. Phys.* **B14** (4) (1977) 545.
5. G. ROUX, *Physique des Matériaux* (CSTB, Paris, France) **1442** (1977) 40.
6. J. W. SUMMERS, J. D. ISNER and E. B. RABINOVITCH, *Polym. Eng. Sci.* **20** (1980) 155.
7. R. JACOB, GFP Conference on Ageing and Stabilisation of PVC, Lyon, 1981.
8. J. PABIOT and J. VERDU, *Polym. Eng. Sci.* **21** (1981) 32.
9. L. S. BURN, *Polym. Deg. Stab.* **36** (1992) 155.
10. I. JACUBOWICZ and K. MOLLER, *ibid.* **36** (1992) 111.
11. G. E. SCHOOLENBERG, *J. Mater. Sci.* **23** (1988) 1580.
12. L. AUDOUIN, V. LANGLOIS, J. VERDU and J.C.M. DE BRUIJN, *ibid.* **29** (1994) 569.
13. J. VERDU, *J. Macromol. Sci., Pure Appl. Chem.* **A3** (10) (1984) 1383.
14. K. T. GILLEN and R. L. CLOUGH, in "Handbook of Polymer Science and Technology," Vol. 2, edited by N. P. Cheremissof (Marcel Dekker, NY, 1989) p. 170.
15. J. L. GARDETTE, S. GAUMET and J. PHILIPPART, *J. Appl. Polym. Sci.* **48** (1993) 1885.
16. C. ANTON-PRINET, J. DUBOIS, G. MUR, M. GAY, L. AUDOUIN and J. VERDU, *Polym. Deg. Stab.*, in press.
17. C. ANTON-PRINET, G. MUR, M. GAY, L. AUDOUIN and J. VERDU, *Polym. Deg. Stab.*, in press.
18. P. SONDHEIMER, D. A. BEN EFRAIN and R. VOLOWSKY, *J. Amer. Chem. Soc.* **83** (1961) 1675.
19. C. ANTON-PRINET, Thesis, ENSAM Paris, 1996, and publications to appear.
20. O. SAÏTO, in "The Radiation Chemistry of Macromolecules," edited by M. DOLE (Academic Press, NY, 1972).
21. P. MOREL, G. MAROT and P. DELPRAT, Paper Presented in 11 ièmes Journées sur le vieillissement Bandol, France, 1995.
22. R. GRECO and G. RAGUSTA, *Plast. and Rubb. Process. Appl.* **7** (1987) 163.
23. A. A. GRIFFITH, *Philos. Trans. R. Soc.* **A211** (1921) 163.
24. E. M. ARRUDA and M. C. BOYCE, *Polym. Eng. Sci.* **30** (20) (1990) 1288.
25. S. WU, *J. Polym. Sci., Part B, Polym. Phys.* **27** (1989) 723.
26. E. A. DI MARZIO, *J. Res. NBS* **68** (A) (1964) 611.
27. R. P. KAMBOUR, *J. Polym. Sci. Macromol. Rev.* **7** (1973).
28. S. WU, *Polym. Eng. Sci.* **30** (1990) 754.
29. J. M. LEFEBVRE and B. ESCAIG, *Polymer* **34** (3) (1993) 518.

Received 24 March 1997
and accepted 28 July 1998